Effects of time-delayed feedback on chaotic oscillators

Jung-Wan Ryu,[1,2] Won-Ho Kye,[1] Soo-Young Lee,[1] Myung-Woon Kim,[2] Muhan Choi,[1] Sunghwan Rim,[1] Young-Jai Park,[2] and Chil-Min Kim[1,*]

[1]*National Creative Research Initiative Center for Controlling Optical Chaos, Pai-Chai University, Daejeon 302-735, Korea*

[2]*Department of Physics, Sogang University, Seoul 121-742, Korea*

(Received 22 March 2004; revised manuscript received 11 June 2004; published 30 September 2004)

We study the effects of time-delayed feedback on chaotic systems where the delay time is both fixed (static case) and varying (dynamic case) in time. For the static case, typical phase coherent and incoherent chaotic oscillators are investigated. Detailed phase diagrams are investigated in the parameter space of feedback gain (K) and delay time (τ). Linear stability analysis, by assuming the time-delayed perturbation, varies as $e^{\lambda t}$ where λ is the eigenvalue, gives the boundaries of the stability islands and critical feedback gains (K_c) for both Rössler oscillators and Lorenz oscillators. We also found that the stability island are found when the delay time is about $\tau=\left(n+\frac{1}{2}\right)T$, where n is an integer and T is the average period of the chaotic oscillator. It is shown that these analytical predictions agree well with the numerical results. For the dynamic case, we investigate Rössler oscillator with periodically modulated delay time. Stability regimes are found for parameter space of feedback gain and modulation frequency in which it was impossible to be stabilized for a fixed delay time. We also trace the detailed routes to the stability near the island boundaries for both cases by investigating bifurcation diagrams.

DOI: 10.1103/PhysRevE.70.036220 PACS number(s): 05.45.Gg, 05.45.Pq

I. INTRODUCTION

The time-delayed chaotic systems have attracted much attention recently since the delay time is inevitable in nature due to the finite propagation speed. It is well known that the effect of time delay is mainly twofold. On the one hand, the delay time on a low dimensional chaotic system increases the embedding dimension and the number of positive Lyapunov exponents of the system. As a result, it leads the system to a hyperchaotic one [1–10]. On the other hand, the time delay on chaotic system also suppresses the chaoticity of the system, e.g., control to the unstable periodic orbits of the chaotic trajectory [11], the stabilization of the unstable fixed point (control to steady state), and amplitude death phenomenon [12,13]. In this study, we concentrate on the latter case since it is practically more useful.

As early as the middle of the nineteenth century Lord Rayleigh observed the suppression of oscillations of interacting systems in two side-by-side standing organ pipes of the same pitch [14]. Since then, this phenomenon has been referred to as *quenching effect* or *oscillation death.* It is known that when the coupling strength is sufficiently strong and the distribution of the natural frequencies of the oscillators is sufficiently broad, the amplitude of the oscillators can be suppressed to zero [15–17]. Recently, the same phenomenon was observed in diffusively coupled chaotic oscillators when the coupling strength and the frequency detuning were sufficiently large [18–20]. The phenomenon is also reported in inhomogeneous oscillating medium by the effect of stirring [21] and even in small-world networks [22].

Recently, the phenomenon of oscillation death has been focused on the time-delayed coupling in limit-cycle oscillators [12]. It has been reported that the amplitude of the time-delay coupled limit-cycle oscillators can shrink to zero at the proper coupling strength and delay time [23]. This phenomenon, named amplitude death, which is defined as the cessation of oscillation of two or more coupled systems as a results of their interaction, was demonstrated in experiment with coupled electronic circuits [23] and coupled thermo-optical oscillators [24]. The effect of distributed time delay was also studied and reported in the context of coupled limit-cycle oscillators [25]. The impact of time-delayed self-feedback on the limit-cycle oscillator was also studied [26]. The results show that time-delayed self-feedback also leads the system to steady state, which is similar to amplitude death phenomenon, for a certain value of delay time and feedback gain.

One notable feature of the time-delayed effect is that amplitude death can occur even if the natural frequencies of the limit-cycle oscillators are identical, in contrast to the case without time-delay in which broad distributions in the natural frequencies of the oscillators are indispensable to amplitude death. Despite the fact that many studies have been done on the amplitude death phenomenon with time-delayed coupling so far, most of the studies were focused on limit-cycle oscillators. In a broad sense, the amplitude death phenomenon is quite similar to the problems of control to steady state, i.e., an unstable fixed point, since a simple homeomorphism always can transform an unstable fixed point to the origin. Many studies [27–31] have been done on the control to unstable periodic orbits in the context of delay time since the pioneering work of Pyragas was published in 1992 [32]. Recently the impact of time-delayed feedback was studied both numerically [33] and experimentally [34]. In Ref. [33], the authors showed that control to steady state as well as unstable periodic orbits is possible for an autonomous system with Lorenz-like chaos, i.e., a single mode laser.

*Electronic address: chmkim@mail.paichai.ac.kr

This paper is organized as follows. In Sec. II, we have investigated the self-feedback effect of static time delay on the Rössler and the Lorenz oscillators, which are the typical coherent and incoherent chaotic oscillators. By investigating linear stability near the unstable fixed point of the Rössler oscillator, we have obtained stability islands regions in the parameter space of feedback gain and delay time, and confirmed them numerically. In Sec. III, we study dynamic time delay feedback effect on the Rössler oscillator. The stability parameter regimes are shown. Finally, we conclude in Sec. IV.

II. STATIC TIME DELAY

A. Coherent chaotic oscillator: Rössler oscillator

For the first example, we study the Rössler oscillator, which is a typical coherent chaotic oscillator, to investigate the amplitude death phenomenon. The time-delayed feedback is introduced as follows:

$$\dot{x} = -\omega_0 y - z + K[x(t-\tau) - x(t)],$$

$$\dot{y} = \omega_0 x + a y + K[y(t-\tau) - y(t)],$$

$$\dot{z} = b + z(x-c) + K[z(t-\tau) - z(t)], \tag{1}$$

where τ is the delay time, K is the feedback gain, and the parameters a, b, c, and ω_0 are 0.15, 0.2, 10.0, and 1.0, respectively. Assuming the linear perturbation varies $e^{\lambda t}$, where λ is the eigenvalue, we obtained the following equation through linear stability analysis of Eq. (1) near the unstable fixed point of the unperturbed oscillator:

$$\begin{pmatrix} A & -1 & -1 \\ 1 & a+A & 0 \\ z_f & 0 & x_f - c + A \end{pmatrix} \mathbf{x} = \lambda \mathbf{x}, \tag{2}$$

where $A = K(e^{-\lambda\tau} - 1)$, $\mathbf{x} = (x\ y\ z)^T$, x_f and z_f are the coordinates of the unstable fixed point, given by $x_f = (c - \sqrt{c^2 - 4ab})/2$, and $z_f = (c - \sqrt{c^2 - 4ab})/2a$. From the above equation, we obtained the characteristic eigenvalue equation that is given as follows:

$$(x_0 - c + A - K - \lambda)[(A - K - \lambda)(a + A - K - \lambda) + 1] - z_0(a + A - K - \lambda) = 0. \tag{3}$$

On the boundaries of the stability islands, the eigenvalue λ become pure imaginary, $\lambda = i\beta$. Equation (3) implies two equations. The boundaries of the stability islands can be obtained from the equation $f(K,\tau) = 0$ by eliminating β. The solid lines in Fig. 1 are the result of this linear stability analysis. We have found only three islands around $\tau = (n + \frac{1}{2})T$ $(n = 0, 1, 2)$ for given system parameters of the Rössler case, where T is the period corresponding to the natural frequency ω_0. The size of the island is reduced as the delay time increases. We have noticed that the perburbation term A in Eq. (2) appears only on the diagonal part, which means the eigenvalue λ_0 of the unperturbed oscillator is closely related to the eigenvalue λ of the perturbed one. From this relation

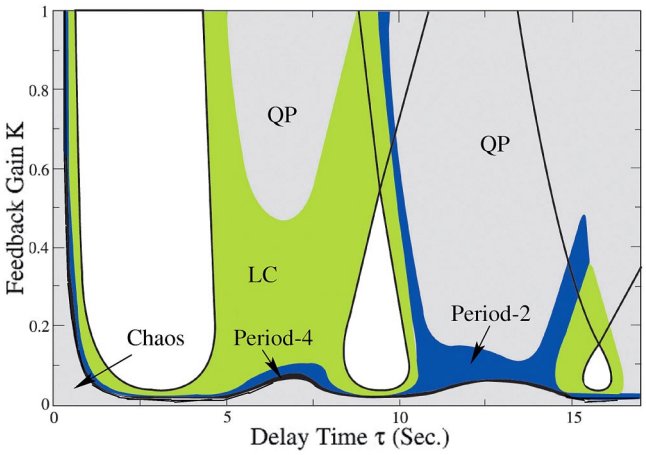

FIG. 1. Phase diagram of the time-delayed feedback Rössler oscillator. The solid line is the analytically obtained boundary of the stability islands (white regions). Other regions are obtained numerically. Notice that the islands are surrounded by the region of limit cycle. LC and QP represent limit cycle and quasiperiodic region, respectively.

we can estimate the critical feedback gain K_c below which stabilization of the fixed point cannot be achieved. The relation is

$$K_c = \frac{1}{2}\mathrm{Re}(\lambda_0), \tag{4}$$

in the present case, $\lambda_0 \sim 0.076$, therefore $K_c \sim 0.038$. The analytical result of K_c agrees well with the numerical one (see Fig. 1).

We also numerically studied Eq. (1) in the parameter space of feedback gain and delay time. The result is shown in Fig. 1. Notice that the stability islands are almost exactly matched with the analytically obtained boundaries (solid lines). In this phase diagram, all three stability islands are surrounded by limit cycle regions. This implies that the stability is developed from the limit cycle through Hopf bifurcation. Outside the limit cycle regions a period-2 or quasiperiodic orbit appears. We also found period-4, higher-order periodic regions, and a small chaotic regime outside the period-2 orbit.

More detailed regimes of motion can be explored by bifurcation diagrams for a fixed feedback gain K as the delay time varies. Figure 2 shows bifurcation diagrams for $K = 0.3$ and $K = 0.8$. We have taken the positive y values when the trajectory passes $x = 0.0$ on (x,y) space. Figure 2(a) is the diagram from $\tau = 0.0$ to $\tau = 0.8$ for $K = 0.8$ as the delay time increases. The figure shows that chaos transits to a limit cycle through inverse period-doubling bifurcation and the limit cycle transits to steady state. In the bifurcation diagram, we can find periodic windows, chaos, and higher order periodicity. Figure 2(b) is the diagram from $\tau = 4.0$ to $\tau = 6.0$ for $K = 0.8$. The figure shows that the stability regime develops to limit cycles. On further increase of the delay time, the limit cycle develops to quasiperiodicity.

The bifurcation diagram shown in Fig. 2(c) is from $\tau = 8.0$ to 11.0 for $K = 0.3$. In this figure, as the delay time

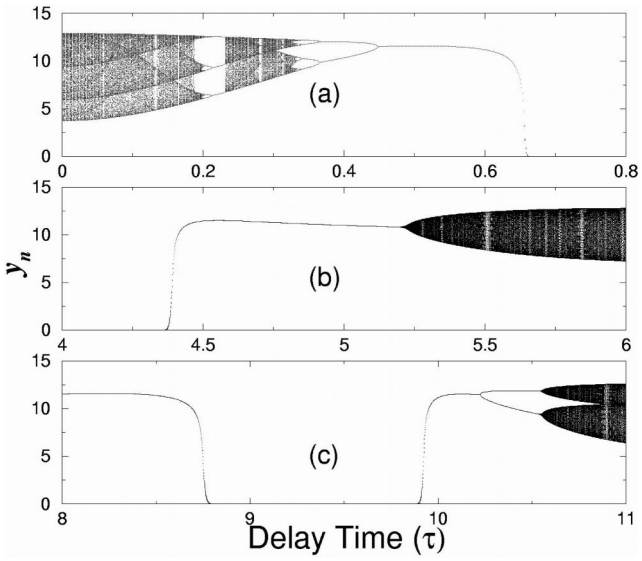

FIG. 2. Bifurcation diagrams depending on the delay time near the stability islands; (a) and (b) are for $K=0.8$ and (c) is for $K=0.3$. These figures show the detailed route to stability islands for a given K.

increases, the amplitude of the limit cycle gradually disappears around $\tau=8.8$, which means it has made the transition to stability. As the delay time is further increased, the dynamics moves from stability region to limit cycle, further bifurcates to a period-2 orbit, and finally develops to a quasiperiodic region. From these bifurcation diagrams, we can understand that the chaotic state of the original system transit to a limit cycle as the delay time increses. When the delay time is longer than the half period of the natural frequency, a limit cycle transits quasiperiodic states through Hopf bifurcation.

In Fig. 3, the time series of steady state, limit cycle, and quasiperiodicity are shown. As seen in Fig. 3(a), for $\tau=0.855$ and $K=0.8$ the chaotic signal converges to a constant value after the time-delayed feedback turned on. Here the constant value corresponds exactly to the y value of the unstable fixed point of the Rössler oscillator. However, when

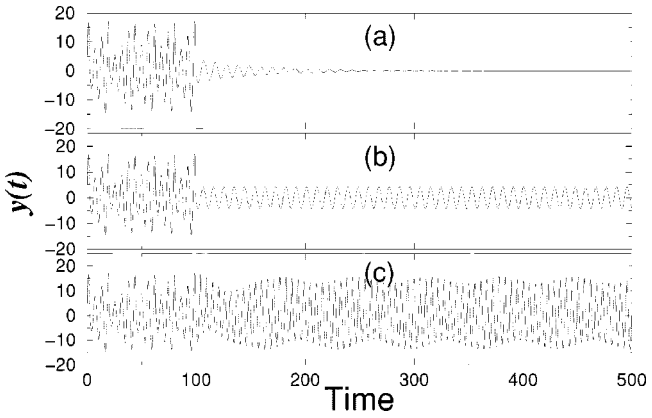

FIG. 3. Time series of the time-delayed self-feedback Rössler oscillator for (a) $\tau=0.855$, (b) $\tau=0.655$, and (c) $\tau=5.5$ for a fixed feedback gain $K=0.8$. Self-feedback is turned on when $t=100.0$.

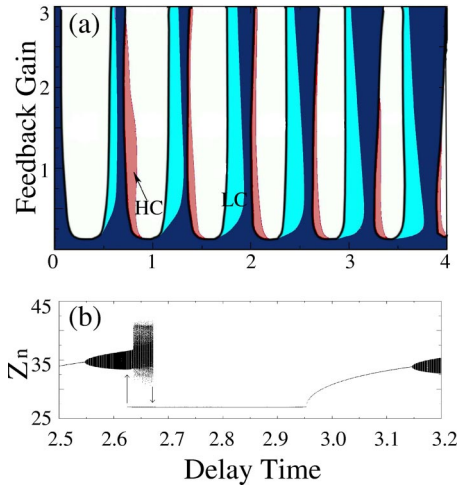

FIG. 4. (a) Phase diagram of time-delayed self-feedback Lorenz oscillator in the parameter space of delay time and feedback gain. (b) Bifurcation diagram as the delay time varies from $\tau=2.5$ to 3.5 for $K=0.5$. The solid black lines in (a) are the analytically obtained boundaries of the islands. White regions, LC, and HC represent stability (steady state), limit cycle, and hysteresis crisis regimes, respectively.

$\tau=0.655$ the chaotic signal changes to a periodic signal as shown in Fig. 3(b). Figure 3(c) shows quasiperiodicity for $\tau=5.5$ and $K=0.8$ that develops from the limit cycle. We confirmed the quasiperiodicity from the spectral analysis and its phase portrait.

Notice that the transition route to stability island (steady state) is via limit cycle motion. This might be expected from the the amplitude death phenomenon of coupled limit cycle oscillators, since coherent chaotic oscillators can sometimes be interpreted as limit cycle oscillators with external noise, and the experimental confirmation of the phenomenon in the limit-cycle case guarantees the robustness of the phenomenon against the small external noise [35].

B. Incoherent chaotic oscillator: Lorenz oscillator

Now, it was of interest to test whether this result holds for incoherent chaotic oscillators. We studied the Lorenz oscillator as the second example. The time-delayed feedback is applied to the z direction as follows:

$$\dot{x} = 10(y - x),$$

$$\dot{y} = 28x - y - xz,$$

$$\dot{z} = -\frac{8}{3}z + xy + K[z(t-\tau) - z(t)]. \tag{5}$$

The linear stability analysis also gives boundaries of the stability islands as in the case of the Rössler oscillator, which are shown as solid lines in Fig. 4(a). Total of 23 islands have been found for given system parameter values. Numerical study of the phase diagram in Fig. 4(a) confirms that the boundaries of the islands are well matched with analytical predictions. The figure shows a part of whole phase diagram

that the stability regions appear when the delay time is approximately equal to $(n+\frac{1}{2})T$ $(n=0,1,\ldots,22)$, like the Rössler oscillator, where T is the period that corresponds to the average frequency of the Lorenz oscillator. As the delay time increases the size of the island is gradually reduced, and eventually the island disappears when the delay time exceeds 14.0.

The bifurcation diagram is shown in Fig. 4(b) over the range of $2.5<\tau<3.5$ for $K=0.5$. The diagram shows the z values that are greater than 27.0 when the oscillator passes $\dot{z}=0.0$ on $(z,\dot{z})$ phase space. As is shown in Fig. 4(b), the steady state, whose value at about 27.0 is exactly matched to that of the unstable fixed point, develops to quasiperiodicity through the limit cycle on the right side as the delay time increases. However, we can find hysteresis regions on the left side of the islands. Between $\tau=2.62$ and 2.67, as the delay time increases, quasiperiodicity transits to chaos and this chaotic band transits to steady state abruptly at $\tau=2.67$, while the steady state transits to quasiperiodicity at $\tau=2.62$ as the delay time decreases. This transition is known as hysteresis crisis [36].

It was in this way that we found the stability islands in the typical incoherent chaotic oscillators. One noticeable property of the Lorenz oscillator in comparison with the Rössler case is that the stability islands is developed via hysteresis crisis on the left hand side boundaries of the islands. In order to check whether this behavior is typical in the case of incoherent chaotic oscillators, we investigated the time-delayed self-feedback Navier-Stokes equation, which is also considered as an incoherent chaotic oscillator. Hysteresis crisis is not found in this case and the stability island is developed from the limit cycle through Hopf bifurcation. This indicates that the appearance of the hysteresis region in Fig. 4 is characteristic of the time-delayed self-feedback Lorenz oscillator rather than a typical behavior of incoherent chaotic oscillator.

Further studies on the time-delayed Rössler oscillator, in which we study the different system parameter values, i.e., $a=0.55$, $b=2.0$, and $c=4.0$, show only one small stability island. We also found several islands in the time-delayed self-feedback Navier-Stokes equation and piecewise linear oscillators [37]. These results imply that the size and number of the islands depends on the kind of chaotic systems as well as on their system parameters. In addition, we also found a similar phenomenon in the case of time-delay coupled chaotic oscillators, e.g., the Rössler and Lorenz case.

III. DYNAMIC TIME DELAY

As a model for the study of a dynamic-time-delayed impact on chaotic systems, we consider the simple case that the delay time is modulated periodically. The generic equation may be written as follows:

$$\dot{\mathbf{x}} = \mathbf{F}(\mathbf{x}, x(t-\tau)),$$

where τ is the delay time that is driven such that $\tau = T_0 \sin(\omega t) + \tau_0$ [10] with $T_0 \leqslant \tau_0$ (const). Here, T_0 and ω are the amplitude and frequency of the delay time. The periodic-time-delayed signal can be fed to the system externally either to a variable or to a parameter. Recently, this periodic-time-delayed chaotic system was proposed to hide the delay time in a communication application [10].

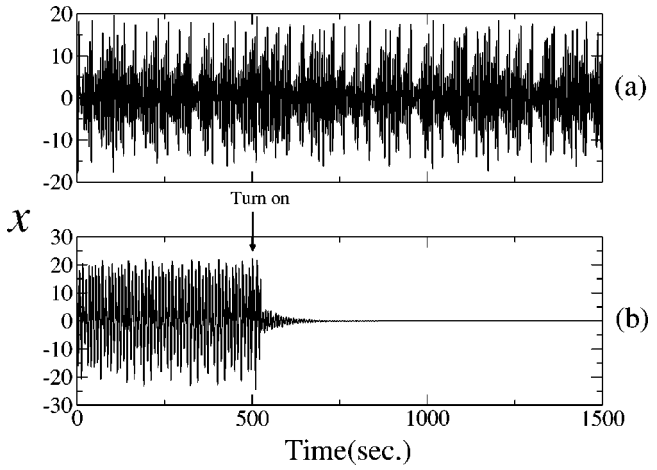

FIG. 5. Time series of $x(t)$ of the periodic-time-delayed Rössler oscillator where its frequency and feedback gain are (a) $\omega=0.2$ and $\beta=0.2$ and (b) $\omega=0.2$ and $\beta=0.42$, respectively.

More explicitly, we study the effect of periodic-time-delayed on chaotic system is done in the following time-delayed Rössler oscillator:

$$\dot{x} = -y - z + \beta[x(t-\tau) - y(t)],$$

$$\dot{y} = x + 0.15\{y + \beta[x(t-\tau) - y(t)]\},$$

$$\dot{z} = 0.2 + z(x - 10.0), \tag{6}$$

where we set $\omega_0=1$ for simplicity. The time-delayed signal $x(t-\tau)$ is fed to the variable y of the form $[x(t-\tau)-y(t)]$, which is more generic form than the previously used form in Sec. II, with the feedback gain β. Throughout this numerical study, we keep the modulation of the delay time as $\tau = 4.5\sin(\omega t)+5.0$.

Figure 5 is the time series of the $x(t)$ depending on the feedback gain β and the modulation frequency ω. When $\beta=0.2$ and $\omega=0.2$, the x variable still exhibits a chaotic signal as shown in Fig. 5(a). However, when we increase β to 0.42 for fixed $\omega=0.2$, the x variable converges to a constant value which corresponds to the unstable fixed point of the variable as shown in Fig. 5(b). In Fig. 5(b), we can see that the oscillator generates irregular signal before the modulation is turned on.

We investigate the stability region as the feedback gain and the driving frequency of the delay time are varied. The dark gray regions in Fig. 6 show stability regions in the parameter space of the feedback gain β and the driving frequency of delay time ω. Note that we cannot observe stability region for constant delay time, i.e., $\omega=0.0$. On the other hand, when we begin to drive the delay time periodically, many stability islands appear, where the chaotic signal collapses to the unstable fixed point. This implies that the periodic driving of the delay time plays an essential role for the

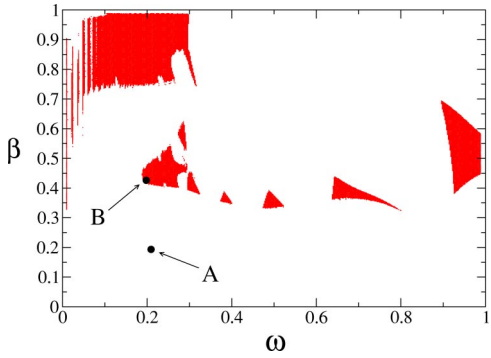

FIG. 6. The stability regions of periodic-time-delayed Rössler oscillator. The dark gray region represents the stability islands. Notice that there is no stability regime at $\omega=0.0$, i.e., for constant time delay. A and B are the reference points to analyze temporal behaviors in Fig. 7.

stabilization. In this sense, we may say that the periodic delay time modulation induces or enhances stablization of an unstable fixed point.

In order to understand the mechanism of this phenomenon, we obtain the distributions of the points $(x(t-\tau),\dot{x}(t-\tau))$ when the trajectory of the Rössler oscillator passes through the Poincaré surface of section $x=0$ ($x>0$ and $\dot{x}>0$) at the time t for two different points in the parameter space, i.e., A (B) which is outside (inside) of the stability region. The results are shown in Figs. 7(b) and 7(d) where θ is defined as the angle between the position of the time delayed signal $(x(t-\tau),\dot{x}(t-\tau))$ and the Poincaré surface of section $x=0$ ($x>0$). For the parameter point A, i.e., $\omega=0.2$ and $\beta=0.2$, the time-delayed signal is spread over the whole range of the angle θ. On the other hand, for B ($\omega=0.2$ and $\beta=0.42$), the distribution has a relatively sharp peak around 1.5π. We can understand, from the result of the periodically modulated time delay Rössler case, that if the angular distribution of the delayed signal is rather coalesced in a certain region, then the delay signal acts as a dragging force to pull the chaotic attractor of the Rössler oscillator to the unstable fixed point. On the contrary, when the angular distribution of the delayed signal is spread on the whole region, there is a

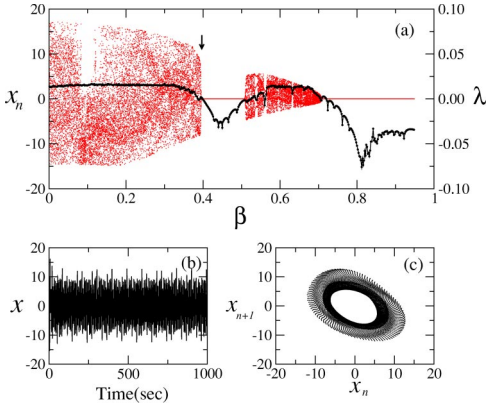

FIG. 8. (a) Bifurcation diagram as the feedback gain is varied for a fixed $\omega=0.2$. The solid line shows the maximal Lyapunov exponent. (b) and (c) are the time series of x and the stroboscopically obtained return map for $\beta=0.39$ [the black arrow in (a)] where quasiperiodic motions are observed. Note that the maximal Lyapunov exponent becomes zero near this regime.

possibility that the direction of the delayed signal trajectory coincides with the direction of the Rössler oscillator trajectory. Then, the trajectory of the Rössler oscillator is pushed out from the unstable fixed point by the delay time so that the system cannot converge to the unstable fixed point.

The detailed transition routes between the stability islands can be investigated by bifurcation diagrams. Figure 8(a) shows a bifurcation diagram as the feedback gain β is varied for a fixed $\omega=0.2$. The bifurcation diagram portrays the transition from a broad chaotic band to a fixed point at $\beta=0.41$, from the fixed point to another band at $\beta=0.51$ and from the band to a fixed point at $\beta=0.72$. To investigate the route more closely, we have calculated the maximal Lyapunov exponent along the parameter values of the bifurcation diagram, which is shown as a solid line in Fig. 8(a). Near the threshold of the stability regimes [see the arrow in Fig. 8(a)], a quasiperiodic motion is observed (note that Lyapunov exponent is almost zero). The quasiperiodicity of the trajectory can be seen from the time series and the return map at $\beta=0.39$ in Figs. 8(b) and 8(c). The return map is obtained stroboscopically with frequency ω by taking the values of the

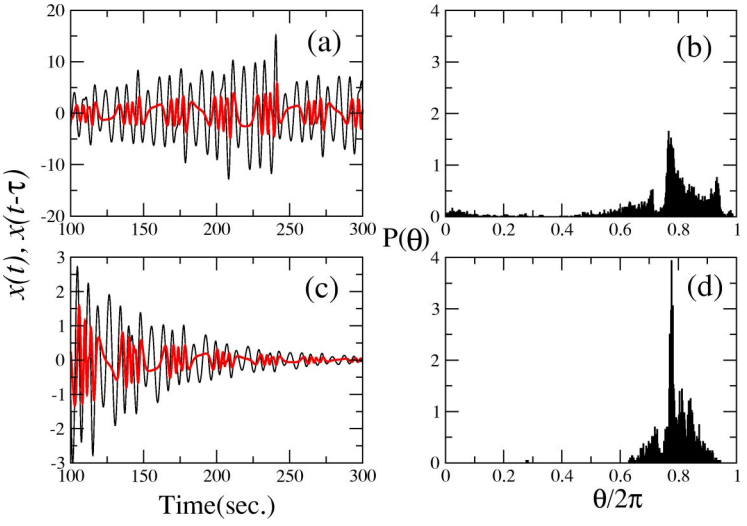

FIG. 7. The time series of $x(t)$ and $x(t-\tau)$ of periodically modulated delay time Rössler oscillator [(a) and (c)] and the angular distributions the delayed signal $(x(t-\tau),\dot{x}(t-\tau))$ [(b) and (d)]. (a) and (b) are for $\omega=0.2$ and $\beta=0.2$. (c) and (d) are for $\omega=0.2$ and $\beta=0.42$.

x variable, which exhibits torus structure [Fig. 8(c)]. This implies that the chaotic behavior transits to stability via quasiperiodicity. This quasiperiodic behavior can be also confirmed by its spectrum and autocorrelation function.

We have also observed this stabilization of the unstable fixed point in various other chaotic systems such as the Lorenz and the Navier-Stokes equations as well as the logistic and the Hénon maps. Even though the system exhibits chaotic trajectories for fixed delay time, the stability regimes are observed for a periodically modulated delay time similar to that of the Rössler oscillator case.

It is interesting to note that this phenomenon does not depend on the specific coupling form, i.e., we can fed a signal of the form $[x(t)-x(t-\tau)]$ or $[y(t)-x(t-\tau)]$ to the systems externally or to a variable of the systems. Especially, when we feed $[x(t)-x(t-\tau)]$ to $\dot{x}$ of the Rössler oscillator externally, the system converges to the unstable fixed point rapidly, where $\tau=10.0\sin(\omega t)+50.0$. In this case, we observe amplitude death in a wide region of $0.0<\omega\leqslant 10.0$, where $\alpha>0.2$. However, for a fixed delay time at $\tau=50.0$, the Rössler oscillator does not exhibit stabilization of the unstable fixed point (see Fig. 1).

IV. CONCLUSIONS

We have studied the effects of both static and dynamic time-delayed feedback on chaotic oscillators (Rössler and the Lorenz oscillators). For the static case, the stability islands are obtained analytically using linear stability analysis and confirmed numerically. We also have found that these islands appear when the delay time is approximately given by $\tau=(n+\frac{1}{2})T$, where n is integer and T is the average period of the chaotic oscillator. From linear stability analysis, we also estimate the critical feedback gain below which the steady state cannot be achieved. Our findings imply that the time-delayed self-feedback signal acts as a dragging force to attract the chaos trajectory to the unstable fixed point of the original chaotic oscillator which is similar to the amplitude death phenomenon of time-delay coupled oscillators. Therefore chaotic motion collapses to the unstable fixed point just by feeding time-delayed signals. We also observed two kinds of routes to the stability island (steady state) for the Lorenz case: one is through Hopf bifurcation and the other through hysteresis crisis, which appear in autonomous systems. For the dynamic case, we have also observed the stabilization regime in the parameter space for time-delayed chaotic systems when the delay time is driven periodically. The behaviors are demonstrated in the Rössler oscillator. In this sense, the periodic modulation of the delay time enhances this phenomenon of the stabilization to the unstable fixed point. Further studies on the dynamic time delay effect, e.g. chaotic or random modulation, on chaotic systems are in progress.

ACKNOWLEDGMENT

This work was supported by Creative Research Initiatives of the Korean Ministry of Science and Technology.

[1] R. He and P. G. Vaidya, Phys. Rev. E **59**, 4048 (1999); L. Yaowen, G. Gguangming, Z. Hong, and W. Yinghai, *ibid.* **62**, 7898 (2000).
[2] T. Heil, I. Fischer, W. Elsässer, J. Mulet, and C. R. Mirasso, Phys. Rev. Lett. **86**, 795 (2001).
[3] D. V. Ramana Reddy, A. Sen, and G. L. Johnston, Phys. Rev. Lett. **85**, 3381 (2000).
[4] V. S. Udaltsov, J.-P. Goedgebuer, L. Larger, and W. T. Rhodes, Phys. Rev. Lett. **86**, 1892 (2001).
[5] J. D. Farmer, Physica D **4**, 366 (1982); K. M. Short and A. T. Parker, Phys. Rev. E **58**, 1159 (1998).
[6] F. T. Arecchi, R. Meucci, E. Allaria, A. Di Garbo, and L. S. Tsimring, Phys. Rev. E **65**, 046237 (2002).
[7] M. C. Mackey and L. Glass, Science **197**, 287 (1977).
[8] M. J. Bünner, Th. Meyer, A. Kittel, and J. Parisi, Phys. Rev. E **56**, 5083 (1997); R. Hegger, M. J. Bünner, H. Kantz, and A. Giaquinta, Phys. Rev. Lett. **81**, 558 (1998); M. J. Buenner, M. Ciofini, A. Giaquinta, R. Hegger, H. Kantz, R. Meucci, and A. Politi, Eur. Phys. J. D **10**, 165 (2000); M. J. Buenner, M. Ciofini, A. Giaquinta, R. Hegger, H. Kantz, R. Meucci, and A. Politi, *ibid.* **10**, 177 (2000); **10**, 177 (2000).
[9] V. I. Ponomarenko and M. D. Prokhorov, Phys. Rev. E **66**, 026215 (2002); C. Zhou and C.-H. Lai, *ibid.* **60**, 320 (1999); B. P. Bezruchko, A. S. Karavaev, V. I. Ponomarenko, and M. D. Prokhorov, *ibid.* **64**, 056216 (2001).
[10] W. H. Kye, M. Choi, M. W. Kim, S. Y. Lee, S. Rim, C. M. Kim, and Y. J. Park, Phys. Lett. A **322**, 338 (2004).
[11] K. Pyragas, Phys. Rev. Lett. **86**, 2265 (2001); O. Lüthje, S. Wolf, and G. Pfister, *ibid.* **86**, 1745 (2001).
[12] K. Bar-Eli, Physica D **14**, 242 (1985).
[13] D. V. Ramana Reddy, A. Sen, and G. L. Johnston, Phys. Rev. Lett. **80**, 5109 (1998).
[14] A. Pikovsky, M. Rosenblum, and J. Kurths, *Synchronization: A Universal Concept in Nonlinear Science* (Cambridge University Press, New York, 2001).
[15] R. E. Mirollo and S. H. Strogatz, J. Stat. Phys. **60**, 245 (1990).
[16] G. B. Ermentrout, Physica D **41**, 219 (1990).
[17] D. G. Aronson, G. B. Ermentrout, and N. Koppel, Physica D **41**, 403 (1990).
[18] G. Osipov, A. Pikovsky, M. Rosenblum, and J. Kurth, Phys. Rev. E **55**, 2353 (1997).
[19] A. Stefanski and T. Kapitaniak, Phys. Lett. A **210**, 279 (1996).
[20] M. Dolnik and I. R. Epstein, Phys. Rev. E **54**, 3361 (1996).
[21] Z. Neufeld, I. Z. Kiss, C. Zhou, and J. Kurths, Phys. Rev. Lett. **91**, 084101 (2003).
[22] Z. Hou and H. Xin, Phys. Rev. E **68**, 055103(R) (2003).
[23] D. V. Ramana Reddy, A. Sen, and G. L. Johnston, Phys. Rev. Lett. **85**, 3381 (2000).
[24] R. Herrero, M. Figueras, J. Rius, F. Pi, and G. Orriols, Phys. Rev. Lett. **84**, 5312 (2000).
[25] F. M. Atay, Phys. Rev. Lett. **91**, 094101 (2003).
[26] D. V. Ramana Reddy, A. Sen, and G. L. Johnston, Physica D

144, 335 (2000).
[27] P. Parmananda, R. Madrigal, M. Rivera, L. Nyikos, I. Z. Kiss, and V. Gáspár, Phys. Rev. E **59**, 5266 (1999).
[28] N. F. Rulkov, L. S. Tsimring, and H. D. I. Abarbanel, Phys. Rev. E **50**, 314 (1994).
[29] K. Pyragas, Phys. Rev. Lett. **86**, 2265 (2001).
[30] K. Pyragas, V. Pyragas, I. Z. Kiss, and J. L. Hudson, Phys. Rev. Lett. **89**, 244103 (2002).
[31] A. Namajuaūnas, K. Pyragas, and Tamaševičius, Phys. Lett. A **204**, 255 (1995).
[32] K. Pyragas, Phys. Lett. A **170**, 421 (1992).
[33] G. Kocinba and N. R. Heckenberg, Phys. Rev. E **68**, 066212 (2003).
[34] R. Dykstra, D. Y. Tang, and N. R. Heckenberg, Phys. Rev. E **57**, 6596 (1998).
[35] H. G. Shuster, *Handbook of Chaos Control* (Wiley-VCH, Weinheim, 1999).
[36] C. Jeffries and J. Perez, Phys. Rev. A **27**, 601 (1983).
[37] C. M. Kim, S. Rim, W. H. Kye, J. W. Ryu, and Y. J. Park, Phys. Lett. A **320**, 39 (2003).